

Spectrophotometric Scanner for Imaging of Paintings and Other Works of Art

G. Antonioli, F. Fermi, C. Oleari, and R. Reverberi

Università di Parma, Dipartimento di Fisica and INFM-Unità di Ricerca di Parma
Parma, Italy

Abstract

A spectrophotometric scanner has been assembled for applications concerning the conservation of paintings and of other works of art with plane surface. Its optical components, that are a lens, a spectrometer and a monochrome matrix CCD digital camera, are arranged in axial configuration.

A frame of the camera allows the image acquisition of a strip of the scene collecting the reflectance spectra of its pixels. The full image is saved as ordered collection of the reflectance spectra of subsequent strips.

The scanner needs only optical geometrical alignment and the usual wavelength calibration. Evaluation of the fidelity of the color reproduction gives very good results. Measurements of the scanner contrast transfer function (CTF) has been carried out for the estimation of its spatial resolution.

Introduction

The optical scanners are an important class of imaging instruments. Owing to their non invasive effects and to their possible use "in situ", they are valued instruments to take images of paintings and of other flat cultural heritage for conservation and restoration purposes. In these cases the comparison of images taken at different times is a crucial point both to make the diagnosis of the pictorial layer and to follow the historical evolution of the paintings. Images taken for such purposes require both a high spatial resolution, a low geometrical distortions and a device independent and high fidelity color measurements.

There is a general agreement about the fact that the most reliable method to measure the color of a painted surface is to take its spectral reflectance,^{1,4} that is a physical quantity of the pictorial layer independent of the measuring instruments. Based on this physical quantity, a digital image can be stored as an ordered collection of the spectral reflectances of its pixels. Among others, spectral images have several advantages such as: 1) the reconstruction of the images in the CIE color space with choice of the illuminants and of the color matching functions (CMF's); 2) the high fidelity reproduction of the images by means of output display such as monitors or printers able to work in a more than trichromatic reproduction methods⁵; 3) the probability that these images will be valuable also in the future because the spectral reflectance factor will be the reference quantity also for the new colorimetric models; 4) the possibility to

check the conservation state of the paintings because a change of the spectral reflectance factor put in evidence the physic-chemical changes of the pictorial layer; 5) the identification of the colorants used by the artists to avoid metameric problems during the restoration.

At the present, the most studied and used method to obtain spectral images is the multispectral technique.^{4,6-9} The starting point of this technique is the measurement of a limited number of spectral reflectance points (6-12) taking images with a set of optical filters of selected wavelengths and bandwidths. The spectral reflectance of each pixel is then recovered by using deconvolution algorithms. This techniques gives good results but has various critical points. A spectrophotometric technique is in principle the best measuring method so we have made an effort to develop a spectrophotometric scanner, which can be transported to work "in situ". In this paper we describe the physical characteristics of the scanner and we show its performances concerning the color measurements and the spatial resolution.

Scanner Description

The optical arrangements of the scanner is shown in Fig. 1. It is made up of a transmission spectrometer (ImSpector V8 manufactured by Specim, Finland) designed for a 2/3 inch CCD sensor is equipped with a 25 μm entrance slit and cover the 400÷780 nm spectral range with a spectral resolution of about 2 nm. The spectrometer is coupled to a monochrome 2/3 inch CCD matrix chill digital camera (Hamamatsu C4742-12bit, 1280×1024 pixels, 9 f/sec) while a collecting lens (Computar TEC-M55 designed for a 2/3 inch sensor) focalizes the painting on the plane of the entrance slit.

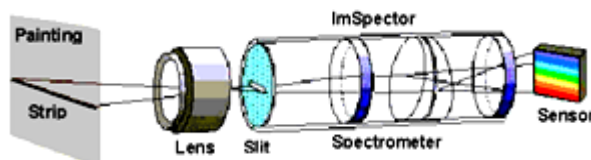


Figure 1. Exploded drawing of the main optical components arranged in the scanner.

The illumination is obtained by means of two 150 W halogen lamps whose light is filtered preventing the illumination of the painting with light of wavelength higher than 750 nm. The light enter into two optical fibers

with blade termination about 30 cm long. The blades can be oriented at 45° with respect to the optical axis of the scanner to obtain a slightly homogeneous horizontal light band 5 cm high and an illuminance of about 30000 lux. The optical parts are firmly mounted on a rigid and massive platform and move rigidly during the scan. Three optical distance sensors allow to set the painting plane perpendicular to the optical axis of the system. Figure 2 shows the mechanical arrangement of the optical system and its main components. The digital camera is interfaced to a PC by means of a 12 bit frame grabber (Mutech MV1000). The PC is equipped with a 2GHz CPU and a RAM of 1.5 GB. A software program drives the scanner, acquires data of a strip of the scene and allows to save its image as a spectral image, as a standard BMP or TIFF image or as an ASCII file, after calculation of the CIE color coordinates based on the CMFs and illuminant, previously selected. The program is implemented to reproduce the colors colorimetrically on a calibrated CRT monitor.

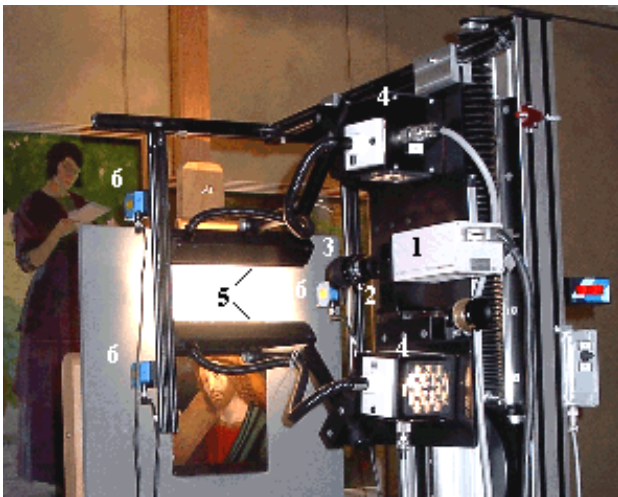


Figure 2. Details of the optical system: 1 digital camera, 2 spectrometer, 3 lens, 4 halogen lamps, 5 fiber blades, 6 distance sensors.

The images are usually captured with $0^\circ/45^\circ$ geometry under these conditions:

- 1) the scanner is free running at a speed of 1.0 mm/sec. This condition allows both to reduce the capture time and to obtain a spatial resolution of about $3.5\div 4.5$ lp/mm as discussed below in the performance section;
- 2) the digital camera is free running at the maximum speed of 9 f/sec, that is, it works with an exposure time of 111 msec;
- 3) the lens is working with a f/8 light stop and magnification by 1/8.

Under these conditions, the scanner takes vertical strip painting area of 7×60 cm² in a scan and a total area of 120×140 cm² in several scans. The painting can be reassembled with a mosaicing program. Of course, the capture conditions can be changed, on occasion. The scanner is rather heavy but it can be disassembled in three parts, transported "in situ", and reassembled easily.

The optical system works as follows (see Figure 1). The lens focalizes the image of a painting surface on the plane of the input slit of the spectrometer, but only the light coming from the strip conjugated with the slit enters into the spectrometer. The light is dispersed by the spectrometer and focalized in the plane containing the sensor of the camera. The spectrometer has a 1:1 image magnification then, the image of the input slit is focalized on the pixel rows of the sensor, while its position along the vertical axis of the sensor, depends on the light wavelength. For examples, if the light entering the slit is red, the image of the slit will be focalized on the top rows of the sensor while if the light is blue it will be focalized on the bottom. White light in the range $400\div 780$ nm entering into the slit fills the whole sensor. Fig. 3 shows schematically how the dispersed light is arranged on the sensor.

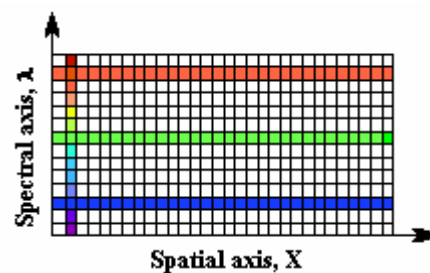


Figure 3. Matrix sensor geometry. The pixel rows of the sensor correspond to a strip of the imaged object at a defined wavelengths while the pixel columns are the spectral signals of the pixels of the imaged strip. The colored rows are three images of the same strip at different wavelengths.

Remembering that the points of the slit are conjugated by the lens with the points of the painting strip, the images of the slit on the sensor are really the images of the strip, then the rows of the sensor define the spatial axis while the columns define the spectral axis. The acquisition of one frame of the digital camera can be thought as the acquisition of the reflectance spectra of each pixels of the strip of the painting. Alternatively, the acquisition of one frame of the digital camera can be thought as the acquisition of as many images of the strip as are the significant wavelengths of the spectrum. Considering the spectral resolution (~ 2 nm) of the spectrometer and the wavelength range of the color measurements ($400\div 730$ nm), we either obtain about 170 spectral points or, alternatively, 170 colored images of the same strip. The above considerations make clear that the presence of the spectrometer changes the matrix camera in a line camera so, to capture the image of a painted surface, it is necessary to scan the painting.

Calibration and Experimental Procedures

The scanner needs two geometrical alignments and a wavelength calibration. First of all, it is necessary to align the spectrometer slit with the pixel rows of the sensor. This operation is rather simple. It needs a spectral lamp lighting a white target. The alignment is made rotating the spectrometer with respect to the camera until the overlap of the reflected light spectra measured by the pixel

columns at the ends of the sensor is obtained. The second alignment operations is obtained rotating the whole optical system until an horizontal line of a target is imaged along the rows of the sensor.

As usual, the wavelength calibration is carried out by measuring the spectra of low pressure lamps such as Hg and Ne lamps. The correspondence between the pixel number and the spectral line wavelengths is nearly linear and allows to calculate the coefficients of a second degree polynomial used for the wavelength calibration. The simple spectral lines of the lamps and a red laser have been also used to evaluate the dependence of the spectral bandwidth of the scanner on the wavelength. This information is useful because a corrected spectral measurement requires a constant bandwidth with a slightly triangular profile. From this point of view the scanner has a satisfactory behavior.

Two general calibrations of the scanner must be carried out before to take spectral images. The first, is a white calibration. This procedure allows to store a low noise spatially averaged reflectance factor, $R_W(\lambda)$, of the standard white used in the calculation of the pixel reflectance during the spectral image measurement. This is necessary to compensate the spatial nonuniformities of the standard white. The second measurement is that of the length of the imaged painting strip under the measurement conditions. This parameter must be written on the specific window of the setup menu of the acquisition program and used to conserve the aspect ratio of the painting. Moreover, it allows to calculate the correct magnification of the lens. These procedures must be carried out when either the standard white or the geometrical conditions of the measurement are changed. Both calibrations are performed by taking the images of the standard white and of a ruler as described below. However, during the white calibration, the certified reflectance factor $R_C(\lambda_n)$ of the standard white, substitute $R_W(\lambda_n)$ in Eq.1.

The measurement of a spectral image of a painting requires four steps:

1. the setup of the main menu of the acquisition program by requiring the choice of the CMF and of the illuminant;
2. the acquisition of a black reference signal frame. It is taken by shuttering the lens and averaging on a selected number of frame signals to reduce the noise;
3. the acquisition of a white reference signal frame. This signal is taken with the standard white reference used for the white calibration discussed before, averaging several frames on space and time. This allows to compensate the spatial nonuniformities of the standard white radiance factor and to reduce the signal noise. Before accepting the white signal frame, the software program displays the maximum signal recorded by the sensor pixels preventing saturation;
- 4) the start of the scanner after the selection of the scan speed and of the number of frame to acquire.

The acquisition program calculate the spectral reflectance of the pictorial layer for any pixel of the sensor in agreement with the equation:

$$R_m(\lambda_n) = R_W(\lambda_n) \frac{S_{nm} - B_{nm}}{S_{W,nm} - B_{nm}} \quad (1)$$

where the indices nm indicate the coordinate of the pixel sensor. Remembering that the column m and the row n of the sensor correspond respectively to the pixel m of the imaged strip of the painting and to the wavelength λ_n , $R_m(\lambda_n)$ is the reflectance factor at wavelength λ_n of the pixel m of the imaged strip; $R_W(\lambda_n)$ is the spatially average spectral radiance factor at wavelength λ_n obtained with the white calibration procedure; S_{nm} , $S_{W,nm}$ and B_{nm} , are the signals measured at the pixel nm of the sensor due to the light reflected by the layer and by the standard white and the black signal, respectively.

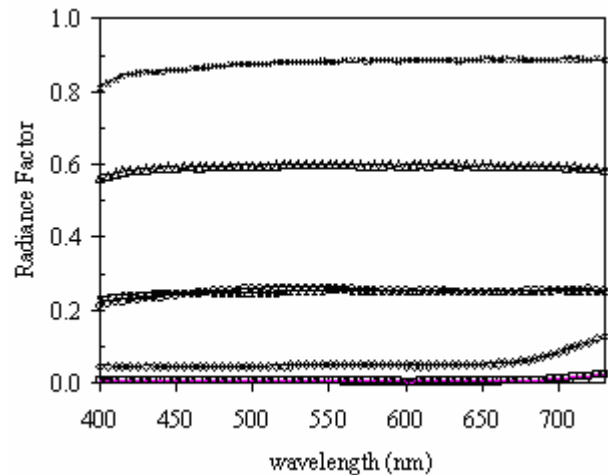


Figure 4. Linearity of the scanner spectral responsivity. The measurement have been performed by using the grey and the white and the black NPL tiles: (x) white, (Δ) pale grey, (*) mid grey, (\circ) difference grey, (\diamond) deep grey, (\square) black. Full line are the measured reflectance factors

Provided that the scanner has a linear response, by using this technique we can assume that the measurement of the surface reflectance factor does not depend: 1) on the spectral irradiance of the lighting system; 2) on the nonuniformity of the spatial irradiance; 3) on the optics spectral transmission; 4) on the spectral responsivity of the scanner. The linearity of the system has been evaluated by taking the spectral images of the grey plus the white and the black NPL tiles, covering a light intensity ratio of about 1:250. The spectral reflectance factors we measure are reported in Fig. 4 together with their NPL certificated spectra for a comparison. The measured spectral reflectance factors fit nearly perfectly the certified spectra. Really, in Fig. 4, it is impossible to distinguish the full line of the measured spectra, because they are masked by the marks indicating the certified values of the spectral radiance factors. As a consequence, we can say that the scanner has a good linear response. In this case we can write:

$$\frac{S_{nm} - B_{nm}}{S_{W,nm} - B_{nm}} = \frac{I_{nm} R_m(\lambda_n) T_m(\lambda_n) R_{nm}}{I_{nm} r_{W,m}(\lambda_n) T_m(\lambda_n) R_{nm}} = \frac{R_m(\lambda_n)}{r_{W,m}(\lambda_n)} \quad (2)$$

where I_{nm} and R_{nm} are respectively, the irradiance at pixel m of the painting and the response of the pixel nm of the sensor at wavelength λ_n ; $T_m(\lambda_n)$ is the transmission of the optical components of the light reflected by the pixel m at

wavelength λ_n and $r_{w,m}(\lambda_n)$ is the spatial averaged reflectance factor of pixel m of the standard white at wavelength λ_n corresponding to the white reference signal taken in step 3 of the image capture procedure. The other symbols have been defined previously. Eq.2 supports our initial assumptions because $R_m(\lambda_n)$ depends only on $r_{w,m}(\lambda_n)$.

Equation 2 becomes Eq.1 if $r_{w,m}(\lambda_n)=R_W(\lambda_n)$. We can assume that this equality occurs owing to the spatial averaging performed during both the white calibration and step 3 of the procedure used to capture images.

Estimation of the Scanner Performance

Two main technical specifications of a scanner are its color reproduction and its spatial resolution.

Though the evaluation of the color reproduction of a painting is a complex task involving psychological tests, a technical evaluation of the color reproduction by using standard color sample, gives significant informations on the ability of the scanner to measure colors.

Measurements have been performed on a set of 12 color glossy tiles plus a white and a black glossy tiles supplied by the National Physical Laboratory (UK) with certified spectral radiance factors at $0^\circ/45^\circ$ geometry.

We used the NPL white tile as the white reference standard to capture the spectral images of the tiles arranged in a panel, then we took the spectral radiance factor of the tiles averaging on the central area corresponding to that of the NPL certification. The temperature of the tiles have been measured both before and after the measurements by a laser thermometer and was found about 24°C closed to the 23°C of the certification. The comparison between the measured and the NPL certified spectral radiance factors of the colored tiles, are shown in Fig. 5 where the full line indicate the spectra measured with the scanner while the discrete points are the values of the NPL certified spectral radiance factors. The agreement between the measured and certified spectra is very good. There is a weak disagreement only for wavelength higher than 700 nm and in the blue region. This is significant for the bright yellow and the orange showing radiance factors rising at lower wavelengths. This behavior that we ascribe to stray light, determines the high CIELAB color differences shown in Table 1 clearly due to the high Δb^* . The CIELAB color coordinates have been calculated on the spectral range $400\div 730$ nm, using the measured and the NPL certified spectral radiance factors, by means of the CIE CMFs for the 2° Observer and the illuminants D65 and following the recommended CIE procedure. The color differences according to the CIELAB 76 and the CIELAB 94 formulas have been calculated. These results, summarized in Table 1, put in evidence the good color reproduction it is possible to obtain with the scanner. In fact, a great number of tiles shows a ΔE_{ab} lower or closed to 1 except the bright yellow and the orange as discussed before. Moreover, the color differences ΔE_{94} are all lower than 1 indicating a quite good performance of the scanner that we can specify with the average $\Delta E_{94-AV}=0.49$ and maximum $\Delta E_{94-Max}=0.90$ color differences for D65 illuminant. Obviously, this performance is almost independent on the illuminant used to calculate the colors. The lightness-chroma gives

interesting indications about the ability of the scanner to measure colors. This plot is reported in Fig. 6 showing both the measured and the certified CIELAB coordinate of the NPL tiles, for a comparison.

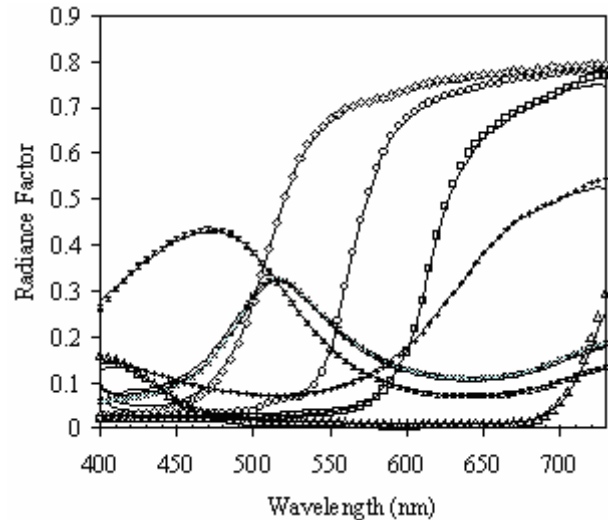


Figure 5. Comparison of the measured and certified spectral radiance factor of the colored NPL tiles. The full lines indicate the measured spectra, discrete points indicate certified values: (\circ) orange, (\square) red, (\diamond) bright yellow, ($-$) green, (\times) difference green, ($+$) deep pink, ($*$) cyan, (Δ) deep blue.

Table 1. CIELAB color differences calculated with 2° Observer and D65 illuminant.

Colours	ΔL^*	Δa^*	Δb^*	ΔE_{ab}^*	ΔE_{94}^*
White	0.01	-0.01	-0.01	0.02	0.02
Black	-0.61	-0.36	0.56	0.90	0.88
Pale Grey	-0.02	0.02	0.03	0.04	0.04
Difference Grey	-0.32	-0.09	-0.17	0.37	0.37
Mid Grey	-0.40	0.04	-0.18	0.44	0.44
Deep Grey	-0.24	-0.18	0.10	0.31	0.31
Deep Pink	-0.34	0.37	-0.39	0.63	0.47
Red	-0.38	0.73	1.00	1.29	0.52
Orange	-0.15	0.58	3.44	3.49	0.89
Bright Yellow	0.22	-0.64	4.05	4.10	0.90
Green	-0.14	-0.91	0.37	0.99	0.38
Difference Green	-0.05	-1.12	0.70	1.32	0.47
Cyan	-0.21	0.49	-0.76	0.93	0.57
Deep Blue	-0.38	1.06	-0.72	1.34	0.66

The first observation is that the reproduction accuracy of the lightness is very good for all colors, while the chroma puts in evidence a slight desaturation going towards the high chroma colors. However, no hue error is put in evidence.

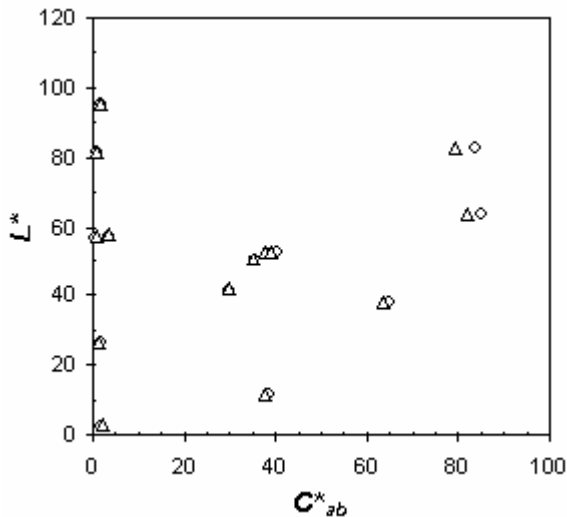


Figure 6. CIELAB Lightness-Chroma plot of the color coordinates of a set of 14 certified NPL tiles for 2° CMFs and D65 illuminant: (○) certified coordinates, (△) scanner measurements.

The spatial resolution of the scanner can be characterized by means of the Contrast Transfer Function (CTF). The CTF accounts for the effects of all the factors lowering the spatial resolution of the scanner when it is taking an image. The simplest method to measure the CTF is to take the images of a test bar target with black and white bar pairs of several spatial frequencies, usually measured in line pair for unit length (lp/mm). We have used the FBI SIQT Scanner Test Chart, supplied by Sine Patterns (USA). This test chart includes two identical set of black and white horizontal and vertical bar pairs with spatial frequencies up to about 20 lp/mm. The scanner test chart is carefully arranged to have the vertical bar sets perpendicular to the entrance slit of the spectrometer, allowing the determination of the horizontal CTF, that is, perpendicular to the scanning direction. Obviously, the horizontal bars of the test chart allow the determination of the vertical CTF, that is, parallel to the scanning direction. The spectral image of the test chart has been carried out under usual working conditions, as reported before, at several scanning velocities. As an example, the image of the vertical bar frequency region, calculated by using the MCFs 2° Observer and D65 illuminant for a scan speed of 1mm/sec, is shown in Fig. 7.

Calculation of the CTFs have been performed using both the radiance factors of the spectral image of the test chart and its calculated bitmap image. 1) For every spatial frequency region we have taken the reflectance spectra averaged respectively on a high number of pixels having minimum and maximum reflectance factors. By using these spectra we calculated the CTFs for the red, green and blue colors and for the lightness. 2) The CTFs have been also calculated by means of the histogram function, available on several image processing program, using images of the test chart as that shown in Fig.7. The histogram allows the accurate determination of the minimum and maximum signals of the frequency regions. This procedure is very helpful for the high spatial frequencies where it is more difficult to evaluate the minimum and the maximum intensities of the pixels.



Figure 7. Image of the vertical test bars of the FBI SIQT test chart taken with a scanner speed of 1mm/sec, calculated using CIE 2° Observer and D65 illuminant. Numbers indicate the frequency regions in lp/mm.

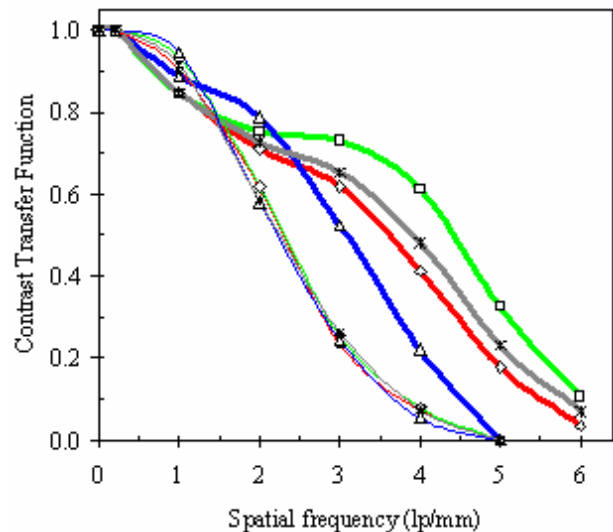


Figure 8. Color CTFs of the scanner obtained from the image of the FBI SIQT test chart taken with a scan speed of 1mm/sec: (—) horizontal CTFs, (---) vertical CTFs; (◇) red, (□) green, (△) blue, (*) lightness. Marks are measured points.

The CTFs obtained with both method are substantially consistent. The results are summarized in Fig. 8 for the image taken with a 1 mm/sec scan speed.

We have also estimated the relative spatial shift of the red, green and blue images plotting the spatial profiles of their signals both for the horizontal and vertical sets of the test bar target. No significant spatial shifts have been found. This means that there isn't evidence of color crosstalk between contiguous pixels.

Figure 8 shows that the red, green and blue colors and lightness vertical CTFs, overlap but are always lower than the horizontal CTFs. The decreasing of the vertical CTFs stops at the spatial frequency of 5 lp/mm. This is physically correct. If we consider that the slit width of the spectrometer is 25 μm and the lens magnification is about 1/8, the lens will focalize exactly on the slit both the white and black bars of a line pair corresponding to the vertical spatial frequency of 5 lp/mm, that is, 200 μm . As a consequence the image of the corresponding area be uniformly grey then we obtain a null CTF. Moreover, they decrease sharply with the increasing of the scan speed. This behavior can be ascribed to the increasing of the spatial integration when the scan speed increases.

Horizontal CTFs is almost independent on the scan speed, as can be foreseen considering that there isn't horizontal spatial integration because there is no motion in this direction. Nevertheless they depend on colors and decrease at higher spatial frequency in the sequence green, red, blue. This behavior is not what we wish for but, at the present, we haven't studied carefully this problem. Then we cannot explain the reasons giving rise to this behavior. On the other hand, our aim was to evaluate the spatial resolution of the scanner and we think we have now significant indications about that. Then, let us to say that, with reference to the Rayleigh criterion R_{10} as in Ref. [10], the vertical spatial resolution can be estimated to be 3.5 lp/mm at a scan speed of 1 mm/sec, while the horizontal spatial resolution can be estimated to be 4.5 lp/mm. This means about 36 lp/mm on the camera sensor, the half of its Nyquist frequency. Probably, this reduction is due to the optical transfer properties of the spectrometer.

On the whole, it seems to us that the spectral resolution of the scanner is close to what is considered the limit of the human eye resolution of 4-6 lp/mm on a A4 sheet viewed at a distance of 25 cm.

Conclusion

Our aim was to develop a prototype of transportable spectrophotometric scanner to be used for archiving and for conservation purposes of work of art. The existence on the market of a spectrometer, developed by Specim (Finland) and to be used in association with the monochrome digital cameras, stimulated us to undertake this task.

We believe this prototype is very promising. As regards to the measurement accuracy of the reflectance factors and consequently of the color specification, its performance is certainly high. Spatial resolution needs improvement and more careful studies but it is close to the resolution of the human eye. The scanner is now under test at the Galleria Nazionale di Parma where we have taken images of paintings by Leonardo, Annibale Carracci, Filippo Mazzola, Jan Provost, Pomponio Allegri, Flemish miniatures and others modern paintings. The images have been highly appreciated by the restorers. Last but not least, the scanner is transportable, simple to calibrate and simple to use.

At the present, the weaker point of the scanner is the image capture time, because about 3 hours are needed for the capture of a 1 m² of painting.

This experience gives us the basis to develop an improved version of this spectrophotometric scanner. The technology development is offering improved version of digital cameras PC's, high speed interfaces, spectrometers, lighting systems, etc. allowing us, we think, to overcome the problems of this scanner we have put in evidence.

References

1. Bernhard Hill, Proc. Of SPIE Vol.3963 Color Imaging: Device-Independent Color, Color Hardcopy, and Graphic Art V, ed. R.Eschbach, G. Marcu, 1999
2. Francisco H. Imai and Roy S. Berns, 9th Congress of the International Color Association Proc. of SPIE Vol. 4421, 2002, pg. 504.
3. Jon.Y. Hardeberg, Francis Schmitt, Hans Brettel, Jean-Pierre Crettez, and Henry Maître, Color Imaging: Vision and Technology Ch. 8, ed. L.W. MacDonald and M.R.Luo, John Wiley (1999).
4. Mark D. Fairchild, Mitchell R. Rosen, Garrett M. Johnson, Munsell Color Science Lab. Technical Report available at <http://www.cis.rit.edu/mcsl/research/reports.html>.
5. Bernhard Hill, 9th Congress of the International Color Association Proc. of SPIE Vol. 4421, 2002, pg. 481.
6. T. Keusen, J. Imaging Sci. and Technol., 40, 510 (1996).
7. Friedhelm König, Werner Praefcke, Proc. CIM 98 Color Imaging in Multimedia, Derby, UK, 1998.
8. Alejandro Ribés, Hans Brettel, Francis Schmitt, Haida Liang, John Cupitt, and David Saunders, PICS'2003 The Digital Photography Conference, Rochester, USA, 2003.
9. S. Tominaga, J. of Electronic Imaging, 8, 332 (1999)
10. Don Williams, Peter D. Burns, PICS'2001, Proc. of the Image Processing, Image Quality, Image Capture System, Montreal, Quebec, Canada, 2001.

Biography

Fernando Fermi received the degree in Physics in 1971 from the University of Parma, Italy. He is Associated Professor of General Physics at the University of Parma. Research has been developed on the photoluminescence properties of semiconductors and insulators. His activity is now mainly devoted to applied spectroscopy. Recent fields of application are: color characterization of phosphors, electroluminescent displays, industrial sorting of plastic bottles based on materials and color and color imaging spectroscopy.